

Spectroscopic and electrochemical properties of ruthenium(II) polypyridyl complexes

Pu-Hui Xie,^a Yuan-Jun Hou,^a Bao-Wen Zhang,^{*a} Yi Cao,^{*a} Fang Wu,^b Wen-Jing Tian^b and Jia-Cong Shen^b

^a Laboratory of Photochemistry, Institute of Photographic Chemistry, the Chinese Academy of Sciences, Beijing, 100101

^b Key Lab for Supramolecular Structure and Spectroscopy, Jilin University, ChangChun, 130023, People's Republic of China

Received 20th September 1999, Accepted 11th October 1999

Luminescent mixed-ligand ruthenium(II) complexes of type $[\text{Ru}(\text{bpy})_2\text{L}]^{2+}$ (where $\text{bpy} = 2,2'$ -bipyridine, $\text{L} = 3,3'$ -dicarboxy- $2,2'$ -bipyridine **1**; $4,4'$ -dicarboxy- $2,2'$ -bipyridine **2**; or $5,5'$ -dicarboxy- $2,2'$ -bipyridine **3**) were synthesized. Their photophysical, acid–base and electrochemical properties were investigated. The emission lifetime for **2** was the longest, and the emission quantum yield was the highest for **2**. This reveals that the positions of the carboxylic acids in the $2,2'$ -bipyridine ligand had an important influence on the photophysical and electrochemical properties of the complexes.

Introduction

Ruthenium(II) polypyridyl complexes have been employed as efficient photosensitizers for the past two decades, due to their chemical stability, redox properties and excited state reactivity.¹ For studying the steric effect of CO_2H groups on the $2,2'$ -bipyridine ligand in the photoelectric conversion of the ruthenium complexes, photosensitizers of *cis*- $[\text{Ru}(\text{dc bpy})_2(\text{NCS})_2]$ type were synthesized ($\text{dc bpy} = 4,4'$ -dicarboxy- $2,2'$ -bipyridine). This complex was shown to be a most efficient photosensitizer. Its maximum incident monochromatic photon-to-current conversion efficiency (IPCE) was greater than 65%. However, such thiocyanate complexes showed very weak luminescence in solution. The emitting state of the above complex had a luminescence quantum yield of only 0.4% (125 K) and a 50 ns lifetime (298 K).² So it is difficult to study photophysical properties of such complexes by general spectral techniques. The spectroscopy and photochemistry of complexes $[\text{Ru}(\text{bpy})_2\text{L}]^{2+}$ have been of particular interest (for example $\text{L} = \text{dicarboxy-}4,4'$ -bipyridine^{3,4}) because of their longer emission lifetimes and higher emission quantum yields. In such mixed-ligand complexes the electron is largely localized on that ligand which is more easily reduced. If this ligand happens to be protonatable, the formation of the MLCT excited state causes significant changes in the acid–base equilibria of the complex, resulting in large shifts in the $\text{p}K_{\text{a}}$ of the complex.⁵ In addition, the photophysical and redox properties of such transition metal complexes can provide important information for the nature of the ground and excited states. So bis($2,2'$ -bipyridine)-($3,3'$ -dicarboxy- $2,2'$ -bipyridine)ruthenium(II) chloride **1**, bis($2,2'$ -bipyridine)-($4,4'$ -dicarboxy- $2,2'$ -bipyridine)ruthenium(II)

chloride **2** as well as bis($2,2'$ -bipyridine)-($5,5'$ -dicarboxy- $2,2'$ -bipyridine)ruthenium(II) chloride **3** were synthesized. Detailed studies on the properties of all the complexes are reported in this paper. The aim of these experiments was to investigate the steric effects on the photophysical and electrochemical properties of the complexes.

Experimental

Spectral measurements

The ^1H NMR spectra were recorded on a Varian Gemini 300 (MHz) spectrometer, element analysis data on an Italian Carloerba 1160 spectrometer, UV-Vis absorption spectra on a Hitachi U-2001 UV/Vis spectrophotometer and emission spectra on a Hitachi 850 fluorescence spectrophotometer with a computer for data collection and analysis. Emission quantum yields were calculated by comparison with the integrated intensity of the emission spectrum of an absorbance-matched solution of $[\text{Ru}(\text{bpy})_3]\text{Cl}_2$ ($\Phi_{\text{em}} = 0.042$)⁶ in water. The emission lifetimes were measured with a time-resolved spectrofluorimeter (Horiba NAES-1100), based on the single-photon-counting method. The light source (2 ns, full width half maximum, FWHM) for the excitation was a high pressure hydrogen flash lamp of free-running type. Each sample was bubbled with N_2 for 30 min before use.

Acid/base titration experiments

Acid/base titration experiments were performed on samples dissolved in 1 M NaCl solutions to keep a constant ionic strength. The ground state $\text{p}K_{\text{a}}^0$ were determined by spectro-

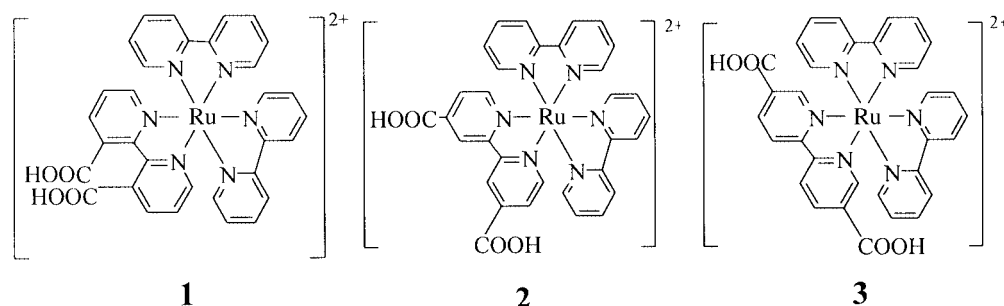


Table 1 Absorption and emission data for the ruthenium polypyridine complexes

| Complex | Solvent | $\lambda_{\text{abs}}^{\text{max}}/\text{nm}$ | $\lambda_{\text{em}}^{\text{max}}/\text{nm}$ (RT) | τ/ns (RT) | ϕ (RT) |
|--|--------------------|---|---|-----------------------|-------------|
| 1 [Ru(bpy) ₂ (3,3'-dcbpy)] | water (pH 7) | 453 | 615 | 109 | 0.012 |
| | CH ₃ CN | 453.5 | 607 | 235 | 0.008 |
| | EtOH | 450 | 601 | 241 | 0.017 |
| 2 [Ru(bpy) ₂ (4,4'-dcbpy)] | water (pH 7) | 459 | 628 | 471 | 0.031 |
| | CH ₃ CN | 457 | 604 | 630 | 0.022 |
| | EtOH | 454 | 597 | 313 | 0.039 |
| 3 [Ru(bpy) ₂ (5,5'-dcbpy)] | water (pH 7) | 450 | 650 | — | 0.0004 |
| | CH ₃ CN | 456 | 606 | — | 0.0005 |
| | EtOH | 456 | 600 | — | 0.0003 |

metric titration, and the excited state pK_a^* by emission titration. The acidities of these solutions were adjusted by addition of dilute HCl and/or NaOH. The pH values were determined using a pH glass electrode. In the strongly acidic regimes, absorption spectra were obtained by titrating with 98.6% H₂SO₄. Estimated errors were as follows: absorption and emission maxima, ± 1 nm; emission lifetime, $\pm 10\%$; pK_a , pK_a^* , ± 0.1 .

Cyclic voltammetry measurements

Cyclic voltammetry measurements were made with HPD-IA equipment. Millimolar solutions of the compounds were prepared in 0.1 M acetonitrile solutions of tetra-*n*-butylammonium tetrafluoroborate. The acetonitrile was freshly distilled over P₂O₅, and the solutions were deaerated by purging with N₂ over 25 min. All voltammograms were recorded under a N₂ atmosphere with a platinum microcylinder working electrode, a platinum wire auxiliary electrode, and a standard calomel reference electrode. Cyclic voltammetry of the ferrocene–ferrocenium redox couple was performed after each experiment to calibrate the pseudo-reference electrode.

Preparations

3,3'-Dicarboxy-2,2'-bipyridine(3,3'-dcbpy),⁷ 4,4'-dicarboxy-2,2'-bipyridine(4,4'-dcbpy),⁸ 5,5'-dimethyl-2,2'-bipyridine,⁹ [Ru(bpy)₃]Cl₂,¹⁰ *cis*-[Ru(bpy)₂Cl₂],¹¹ and *cis*-[Ru(4,4'-dcbpy)₂Cl₂]¹ were prepared by the literature methods. 5,5'-Dicarboxy-2,2'-bipyridine(5,5'-dcbpy) was prepared in the same manner as 4,4'-dcbpy.

[Ru(bpy)₂(3,3'-dcbpy)]Cl₂ 1. The compounds *cis*-[Ru(bpy)₂Cl₂] (160 mg, 0.33 mmol) and 3,3'-dcbpy (101 mg, 0.42 mmol) were refluxed in water–EtOH (20 ml, 1:1 v/v) under N₂ in the dark for 8 h. The product was purified on a neutral alumina column using CH₃CN as eluent. Calc. for **1**·12H₂O: C, 40.68; H, 5.08; N, 8.89. Found: C, 41.20; H, 4.99; N, 8.58%. ¹H NMR (D₂O): δ 8.53 (d, 4 H), 8.27 (d, 2 H), 8.05 (m, 4 H), 7.78 (d, 2 H), 7.66 (d, 2 H) and 7.40 (m, 8 H).

[Ru(bpy)₂(4,4'-dcbpy)]Cl₂ 2. This complex was synthesized as described.¹² Calc. for **2**·4H₂O: C, 48.48; H, 4.00; N, 10.50. Found: C, 48.50; H, 4.01; N, 10.52%. ¹H NMR (D₂O): δ 9.25 (d, 2 H), 8.83 (d, 4 H), 8.30 (d, 2 H), 8.22 (ddd, 4 H), 8.04 (t, 4 H), 7.95 (dd, 2 H) and 7.57 (m, 4 H).

[Ru(bpy)₂(5,5'-dcbpy)]Cl₂ 3. The compound *cis*-[Ru(bpy)₂Cl₂] (160 mg, 0.33 mmol) was mixed with 5,5'-dcbpy (101 mg, 0.42 mmol) in 20 mL of EtOH–water, refluxed for 12 h under N₂ and then concentrated. The solid was recrystallized from MeOH–diethyl ether. Calc. for **3**·2H₂O: C, 50.26; H, 3.66; N, 10.99. Found: C, 50.29; H, 3.60; N, 10.93%. ¹H NMR (D₂O): δ 8.64 (d, 2 H), 8.54 (m, 6 H), 8.13 (d, 2 H), 8.06 (m, 4 H), 7.75 (d, 4 H) and 7.42 (m, 4 H).

Results and discussion

UV-Vis spectra and the ground state pK_a^0 of complexes **1**, **2**, **3**

Absorption spectral data for compounds **1**, **2**, **3** are reported in

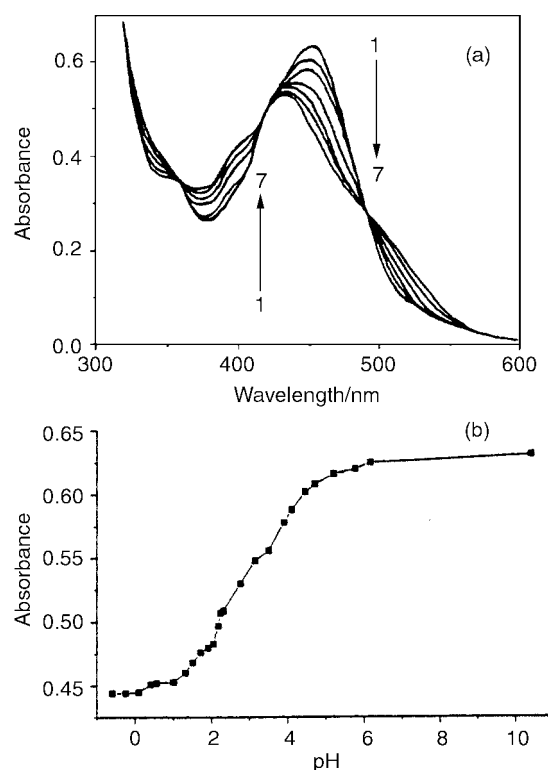


Fig. 1 (a) Absorption spectra of complex **1** in aqueous solution for various values of pH. From 1 to 7: 6.16; 4.7; 4.15; 3.14; 2.6; 2.3; 2.11. (b) Spectrophotometric titration of **1** showing absorbance change at 453 nm for various values of pH.

Table 1. For all the mixed-ligand complexes the low-energy metal-to-ligand charge-transfer (MLCT) band was located anywhere between 450 and 460 nm, being little dependent on the nature of the spectator ligand L and that of the solvent.

The UV-Vis absorption spectra for complex **1** in aqueous solution as a function of pH are shown in Fig. 1(a). As the pH decreased the absorbance of the MLCT band decreased and broadened, then a new, low-energy shoulder appeared at *ca.* 500 nm. The changes of these spectra were completely reversible, and the compound was stable at each pH. There were two isosbestic points at 427 and 496 nm between pH 2 and 7. Below pH 2 the spectra changed little.

The absorption changes at 453 nm as a function of pH between -0.6 and 10.5 for complex **1** showed two inflection points ($pK_{a1}^0 = 0.2$ and $pK_{a2}^0 = 2.2$) in Fig. 1(b) (because the protonation steps were close together, it was not possible to draw good sigmoidal curves to determine pK_a ; the acidity at which the rate of change in absorbance is greatest was chosen to calculate the pK_a for each protonation step¹³). Thus in Fig. 1(b) the spectrum at pH 4.7 represented that of the deprotonated form; at pH 1.9, the monoprotonated form; at pH 0, the diprotonated form. The observations of two isosbestic points and two inflection points in the titration plot demonstrated that two different protonation steps occurred for **1**, eqns. (1) and (2),

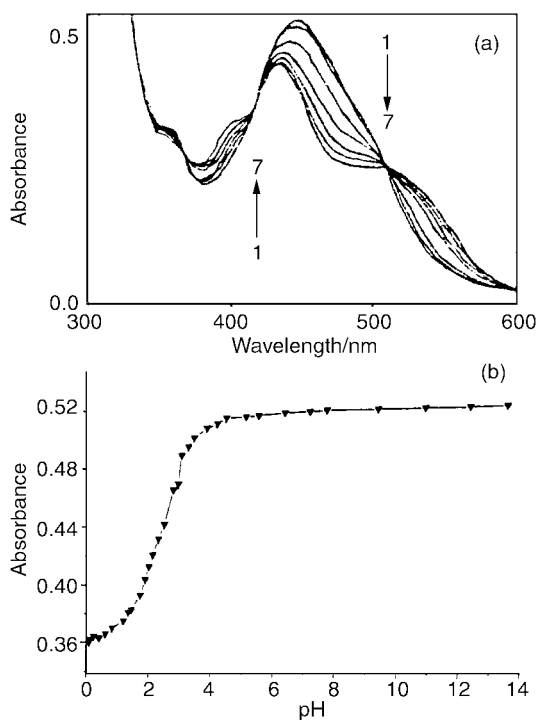
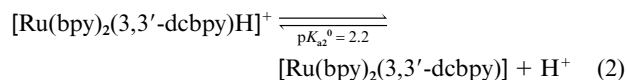
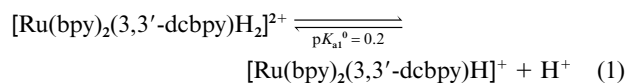


Fig. 2 (a) Absorption spectra of complex **3** in aqueous solution for the following values of pH: 1, 5.48; 2, 3.39; 3, 2.75; 4, 2.11; 5, 1.72; 6, 1.09; 7, 0.83. (b) Spectrophotometric titration of **3** showing the absorbance change at 450 nm for various values of pH.



which could be used to describe the acid/base behavior of this complex.

Protonation of complex **2** also led to a large perturbation of the absorption spectra. Upon lowering of pH the MLCT band located at 459 nm showed a small decrease in intensity. Two isosbestic points at 422 and 478 nm were also found at pH between 1 and 6. Below pH 1 the spectra shifted slightly off the isosbestic but otherwise changed little. The absorption changes at 459 nm as a function of pH between 1 and 11 yielded two $\text{p}K_{\text{a}}$ values for the ground state as 1.7 and 2.9.

Over the pH range 13.0–5.5 the absorption spectra of complex **3** were pH independent. Below pH 5.5 lowering of pH led to significant spectral changes. Fig. 2(a) presents absorption spectra of the fully deprotonated and protonated forms of the complex. The MLCT absorption maximum located at 450 nm was red shifted, and a shoulder appeared at 507 nm with slight decrease in intensity with decreasing pH. Fig. 2(b) shows such a fit for analysis at 450 nm with a single $\text{p}K_{\text{a}2}$ at 3.0 ($\text{p}K_{\text{a}1}$ was below 0.8).

The stronger acidity of complex **1** as compared to its 4,4'-dcbpy and 5,5'-dcbpy analogs could be explained in terms of intramolecular hydrogen-bonding interaction between the two carboxy acid substituents in 3,3' positions. The hydrogen bonding interaction could occur between one of the oxygen atoms bonded to the carbonyl carbon atom in the 3 position on the bipyridine ring with the hydrogen atom bonded to the carboxy group in the 3' position. The distance of the 3,3' positions might fall within the hydrogen-bonding domain, and be more favorable than the 4,4' and 5,5' positions. The hydrogen-bonding interaction might withdraw the electron from the carboxy groups, and would decrease the electron density on the

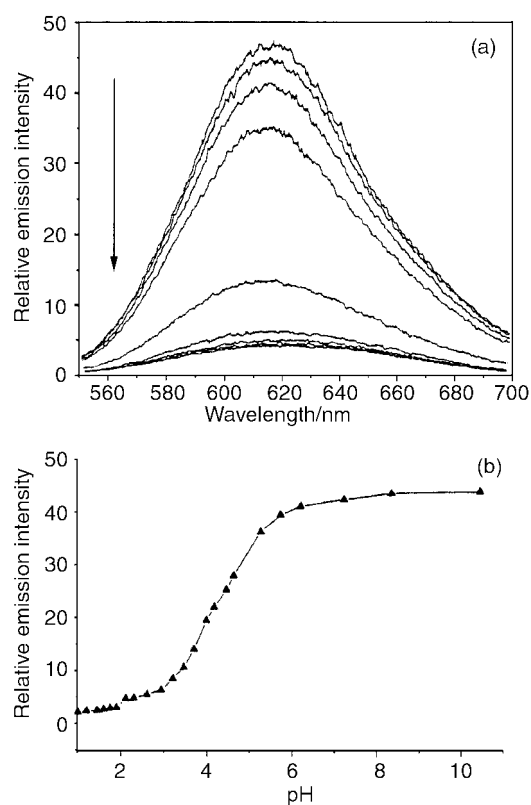


Fig. 3 (a) pH dependence of emission for complex **1**. From 1 to 9, the values of pH are 10.47; 6.16; 4.70; 4.15; 3.14; 2.60; 2.30; 2.11; 1.90 respectively. (b) Titration curve for relative emission intensity with pH for **1** (at 615 nm).

carboxy group and increase the acidity of **1**. So the $\text{p}K_{\text{a}}$ values of **1** were accordingly smaller than those of the other two. However, the hydrogen bonding between the CO_2H groups in the C3 and C3' positions had less influence on the ^1H NMR spectra than the OH groups in the same positions,¹⁴ as two CO_2H substituents of the ligand formed an intramolecular $\text{O}-\text{H}\cdots\text{O}$ hydrogen bonding in a twisted manner, while two OH groups form a six- or seven-membered ring which was more stable.

Complex **3** was the least acidic among the compounds as seen from the above analysis. A possible reason for this was the increase in electron density on the 5,5'-dcbpy positions. Therefore, there was a substantial decrease in the ground state $\text{p}K_{\text{a}2}$ upon going from 5,5'- to 4,4'- and 3,3'-based dyes.

Emission properties

Fig. 3(a) shows the emission spectra for complex **1** under various pH conditions. The luminescence intensity was almost pH independent above pH 7. The emission intensities of **1** varied mildly in dilute acidic solutions. The intensity decreased rapidly in medium acidic solutions and was almost unchanged in strong acid (below pH 2). The luminescence peak at 615 nm in solutions of pH 6.17 and at 635 nm in pH 1.9 were assigned to the deprotonated and monoprotonated forms of **1** in the excited state respectively, suggesting that proton transfer occurred within the emission lifetime of the excited state. The emission intensity of the monoprotonated form was very weak (*ca.* 7%) as compared to that of the deprotonated one.

As for complex **2**, at pH above 5.38, the emission maxima and intensities were independent of pH. When the pH decreased from 5.38 to 4.25 a sudden decrease in intensity occurred. Then between pH 4.25 and 2.99 the emission intensities decreased slowly; at pH below 2.99 the emission maxima and intensities were again almost independent of pH. As the pH decreased from 5.38 to 2.72 the luminescence peak of **2** at 628 nm red shifted to 665 nm, which was assigned to the excited

Table 2 The emission quantum yields and lifetimes at different pH for ruthenium complexes ($\lambda_{\text{ex}} = 454$ nm, $\lambda_{\text{em}} = 610$ nm for **1**, $\lambda_{\text{ex}} = 460$ nm, $\lambda_{\text{em}} = 630$ nm for **2**, $\lambda_{\text{ex}} = 450$ nm, $\lambda_{\text{em}} = 650$ nm for **3**)

| Compound | pH | τ/ns | $10^{-3} \phi_{\text{em}}$ |
|----------|-------|------------------|----------------------------|
| 1 | 13.38 | 341 | 12 |
| | -0.6 | 77 | 3 |
| 2 | 13.38 | 492 | 30 |
| | -0.6 | 190 | 8 |
| 3 | 13.38 | — | 0.54 |
| | -0.6 | — | 0.30 |

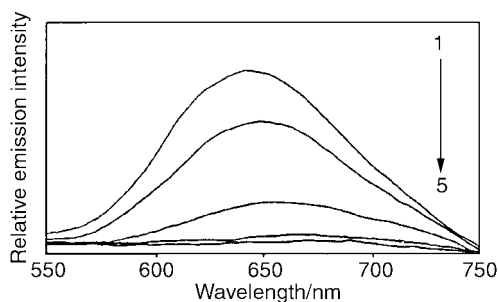


Fig. 4 pH Dependence of emission for complex **3**. From 1 to 5, the values of pH are 5.48, 3.39, 2.75, 2.11, 1.72 respectively.

states of the deprotonated and monoprotonated species respectively.

The effect of variations in pH on the emission spectra vs. intensity of complex **3** are presented in Fig. 4. The fully ionized form, present at $\text{pH} \geq 5.0$, had its emission maximum at 650 nm. The emission was rather weak and short-lived as compared to that of **2**. Lowering of pH led to a decrease in intensity as well as a red-shift to ca. 700 nm at pH 1.7.

A summary of the emission quantum yields and lifetimes of complexes **1**, **2**, **3** at different pH is given in Table 2. The data suggested a profound influence of the positions of the carboxy groups in the 2,2'-bipyridine ligand on the photophysical properties of the complexes. The differences in the emission lifetimes as well as emission quantum yields between these basic and acidic forms in the dicarboxybipyridine chelates were rather significant. The emission lifetimes between the deprotonated and protonated forms were consistent with the emission intensity ratios measured in the steady-state luminescence measurements.

As shown above, complex **1** emitted at shorter wavelength and had a shorter emission lifetime and smaller quantum yield than **2**. This behavior was opposite to the trend predicted by the energy gap law (3)¹⁵ where C is the slope in cm and E_{em} the energy in cm^{-1} at the emission maximum. According to eqn. (3), k_{nr} of **1** should be smaller than that of **2** and therefore

$$K_{\text{nr}} \propto e^{-CE_{\text{em}}} \quad (3)$$

the emission quantum yield of **1** should be higher than that of **2**. This may be attributed to a thermal population of a high-lying ligand field (³LF) state.¹⁶

In general, photoexcitation of ruthenium polypyridyl complexes generates a singlet metal-to-ligand charge-transfer state which undergoes efficient intersystem crossing ($\Phi_{\text{isc}} \approx 1$) to a manifold of closely spaced triplet states (³MLCT).¹⁷ These states can then decay back to the ground state through both radiative (k_r) and non-radiative (k_{nr}) mechanisms, in addition to a thermal population of high-lying ligand field (³LF) states. This ³LF state undergoes fast non-radiative decay to the ground state or ligand dissociation.¹⁸ The energy of the LF excited state depends on the field strength, which depends on the σ -donor and π -acceptor properties of the ligand, the steric crowding around the metal and the bite angle of the polydentate

ligands.¹⁹ For **1** the bite angle cannot be optimized because of the steric hindrance on the 2,2'-bipyridine which leads to weakening of the ligand field strength. Thus, the energy of the LF excited state of **1** decreases. Furthermore, the MLCT energy of **1** is slightly higher than that of **2**. Therefore, k_{nr} increases exponentially with decreasing energy gap between MLCT and LF excited states. In addition, the formation of a hydrogen bond can lead to significant enhancement of non-radiative decay rates. An increase in k_{nr} may be the reason that the quantum yield of **1** is smaller than that of **2**. However, for **3** the longest emitting wavelength and the shortest emission lifetime as well as the smallest emission quantum yield were due to the increase in non-radiative decay rates.

Excited-state emission spectral data on the ruthenium polypyridine complexes examined are also given in Table 1. For all of the mixed-ligand complexes the emission MLCT band was located anywhere between 610 and 700 nm, being much dependent on the positions of the carboxy groups, on the spectator ligand L and the nature of the solvent. In CH_3CN each complex emitted at shorter wavelength than in water; the solvent stabilization of the ³MLCT was ca. 214, 633 and 1117 cm^{-1} for the 3,3', 4,4' and 5,5' Ru complexes respectively. These results showed that solvatochromic shifts in emission can be used to alter the emission energies of $[\text{Ru}(\text{bpy})_2\text{L}]^{2+}$ to produce a solvent-dependent switching.

Excited state $\text{p}K_{\text{a}}^*$

The titration curve of the luminescence intensity at 615 nm for complex **1** in Fig. 3(b) over the pH range of 2–11 shows one inflection point at 3.8. The inflection point represents the equilibrium between the deprotonated form and monoprotonated form and indicates that the pH for the other equilibrium (between monoprotonated and diprotonated form) was lower than 1.9. The results illustrate that the excited complex could be protonated without electronic deactivation. As an example, when the deprotonated form of **1** was excited at pH 3.14 the emission of the monoprotonated form was observed predominantly.

The $\text{p}K_{\text{a}}$ in the excited state ($\text{p}K_{\text{a}}^*$) corresponding to the equilibrium between the deprotonated and monoprotonated form was evaluated in two empirical ways based on Forster's cycle, using the emission and absorption spectra and their titration curves.²⁰ First, in the titration method, the $\text{p}K_{\text{a}}^*$ was given by eqn. (4) where the pH is taken at the inflection point of

$$\text{pH} = \text{p}K_{\text{a}}^* + \log(\tau_{\text{H}}/\tau) \quad (4)$$

1 in the luminescence curve, τ_{H} (102 ns) and τ (341 ns) are the excited state lifetimes of the monoprotonated and the deprotonated species respectively. Then, the $\text{p}K_{\text{a}}^*$ of **1** was determined to be 3.3.

Secondly the Forster treatment results in eqn. (5), which

$$\text{p}K_{\text{a}}^* = \text{p}K_{\text{a}}^0 + (0.625/T)(\nu_{\text{B}} - \nu_{\text{BH}^+}) \quad (5)$$

describes the relationship between ground and excited state $\text{p}K_{\text{a}}$ based on pure 0–0 transitions in wavenumbers (cm^{-1}) for the deprotonated (ν_{B}) and monoprotonated (ν_{BH^+}) forms respectively. At room temperature the ground state $\text{p}K_{\text{a}}^0$ of **1** was 2.2, the emission energy maxima for the deprotonated and monoprotonated species were $\nu_{\text{B}} = 1.63 \times 10^4$, $\nu_{\text{BH}^+} = 1.58 \times 10^4$ cm^{-1} , and the predicted excited state $\text{p}K_{\text{a}}^*$ was 3.2 which agrees well with the value measured by emission titration.

From the titration of the emission intensity at 645 nm for complex **2** over the pH range of 2–11 one inflection point was derived at pH 4.5. According to eqn. (4), and the lifetimes of the deprotonated ($\tau = 471$ ns) and monoprotonated form ($\tau = 243$ ns) of **2**, the $\text{p}K_{\text{a}}^*$ of **2** was 4.2. Using $\nu_{\text{B}} = 1.538 \times 10^4$, $\nu_{\text{BH}^+} = 1.47 \times 10^4$ cm^{-1} , the resulting value of $\text{p}K_{\text{a}}^*$ was 4.3 according to eqn. (5).

Table 3 Data for the ground state and excited state acid–base equilibria in ruthenium polypyridyl complexes

| Compound | p <i>K</i> _a | | p <i>K</i> _{a2} [*] | MLCT (nm) | | Emission λ _{max} /nm | |
|----------|-------------------------|-----|---------------------------------------|-----------|-------|-------------------------------|--------|
| | 1 | 2 | | deprot. | prot. | pH > 7.0 | pH < 0 |
| 1 | 0.2 | 2.2 | 3.3 | 453 | 520 | 615 | 635 |
| 2 | 1.7 | 2.9 | 4.3 | 459 | 500 | 628 | 665 |
| 3 | | 3.0 | 3.5 | 450 | 510 | 650 | 700 |

Table 4 Ground and excited state energies and cyclic voltammetry data for model compounds in CH₃CN^a

| Compound | <i>E</i> _{0,0} ^b /eV | Oxidations ^c | | Reductions | |
|----------|--|----------------------------|---|----------------------------|---|
| | | <i>E</i> _{1/2} /V | <i>E</i> _{1/2} [*] /V | <i>E</i> _{1/2} /V | <i>E</i> _{1/2} [*] /V |
| 1 | 2.18 | 1.29 | −0.89 | −1.53 | 0.65 |
| 2 | 2.25 | 1.27 | −0.98 | −1.50 | 0.75 |
| 3 | 2.26 | 1.26 | −1.00 | −1.44 | 0.82 |

^a All potentials for 10^{−3} M compounds with 0.1 M tetra-*n*-butylammonium tetrafluoroborate as supporting electrolyte. Volts vs. SCE, error in potentials ±0.002 V, *T* = 25 ± 1 °C, scan rate = 100 mV s^{−1}.

^b The values of *E*_{0,0} were obtained from the 298 K emission spectra, it should be noted that *E*_{0,0} cannot be rigorously determined, because of the approximations required in the spectral modelling of the lower frequency modes and the lack of spectral resolution. ^c Mean of cathodic and anodic half-wave potential values.

Fitting of the total emission intensity variation as a function of pH for complex **3** yielded an inflection point (p*K*_a^{*} value) at 3.5. Comparison of similar data for the other two complexes showed that the shift in the p*K*_a upon formation of the MLCT excited state was the least pronounced (Δp*K*_a = 0.5 for **3**, as compared to ≥1.1 for the other two). Table 3 summarizes the absorption and emission properties measured in this work for each dcby complex in the deprotonated and protonated forms.

The higher apparent p*K*_a^{*} values of the compounds as compared to each ground-state p*K*_a value indicated that the excited-state deprotonated forms of each compound were slightly more basic than the ground-state analogue. The higher p*K*_{a2}^{*} value of each complex suggested that the ligand electron density is significantly higher in the excited state than in the ground state, due to the charge transfer transition from metal to ligand. In the excited state the electron was located on the dcby ligand; such redistribution of charge creates more electron density on the carboxy groups, thus causing them to be more basic.

Electrochemical data

Redox potentials for the complexes in CH₃CN were obtained by cyclic voltammetry. Results are listed in Table 4. For these complexes the oxidation corresponds to removal of an electron from the d orbital of Ru^{II} to give Ru^{III}. The reduction corresponds to reduction of the ligand containing the carboxy acid groups. In mixed-ligand complexes like these the electron transition upon optical absorption would occur between the metal center and the ligand which is most easily reducible. The electron-withdrawing character of the carboxy group would shift the reduction potential of the ligand positively relative to that of the unsubstituted bipyridine ligand. From **1** to **3** the oxidation potentials decreased with increasing p*K*_a.

Data presented in the above tables on the complexes with carboxy groups reveal several interesting effects on the Ru→L luminescence. Along the ligand series 3,3', 4,4', 5,5' one can note that: (a) the absorption maxima of deprotonated and monoprotinated forms and the emission maxima of deprotonated forms all blue shift with increasing excited-state lifetime

and emission intensity; (b) the p*K*_{a2}^{*} value for the Ru→L CT emission is larger than each p*K*_a⁰ value; (c) the emission properties are sensitive to “fine tuning” of the excited-state energies.

Conclusion

A series of mixed-ligand polypyridyl ruthenium(II) complexes [Ru(bpy)₂(3,3'-dcby)]²⁺, [Ru(bpy)₂(4,4'-dcby)]²⁺, [Ru(bpy)₂(5,5'-dcby)]²⁺ were designed and synthesized. The ground state p*K*_a and excited state p*K*_a^{*} of [Ru(bpy)₂L]²⁺ type complexes were determined. Complex **3** had the shortest emission lifetime and smallest quantum yield. The strongest acidity of **1** could be attributed to intramolecular hydrogen bonding interaction. Compared to the ground state p*K*_a, the higher value for p*K*_a^{*} revealed that the excited state species was a slightly stronger base than its ground state analogue. The positions of the carboxy groups in the 2,2'-bipyridine ligand had an effect on the photophysical properties of the complexes.

Acknowledgements

The authors wish to thank the NNSFC for financial support (No. 29672034 and 29733100).

References

- 1 M. K. Nazeeruddin, A. Kay, I. Rodicio, R. Humphry-Baker, E. Muller, P. Liska, N. Vlachopoulos and M. Gratzel, *J. Am. Chem. Soc.*, 1993, **115**, 6382.
- 2 S. Ferrere and B. A. Gregg, *J. Am. Chem. Soc.*, 1998, **120**, 843.
- 3 P. J. Giordano, C. R. Bock, M. S. Wrighton, L. V. Interrante and R. F. X. Williams, *J. Am. Chem. Soc.*, 1977, **99**, 3187.
- 4 T. Shimidzu, T. Iyoda and K. Izaki, *Chem. Phys. Lett.*, 1979, **68**, 21.
- 5 A. Kirsch-De Mesmaeker, L. Jacquet and J. Nasielski, *Inorg. Chem.*, 1988, **27**, 4451.
- 6 J. Van Houten and R. J. Watts, *J. Am. Chem. Soc.*, 1976, **98**, 4853.
- 7 F. L. Wimmer and S. Wimmer, *OPPI BRIEFS*, 1983, **15**, No. 5, 368.
- 8 G. Sprintschnik, H. W. Sprintschnik, P. P. Kirsch and D. G. Whitten *J. Am. Chem. Soc.*, 1977, **99**, 4947.
- 9 C. M. Elliott and E. J. Hershenhart, *J. Am. Chem. Soc.*, 1982, **104**, 7519.
- 10 S. Anderson and K. R. Seddon, *J. Chem. Res. (S)*, 1979, 74.
- 11 B. P. Sullivan, D. J. Salmon and T. J. Meyer, *Inorg. Chem.*, 1978, **17**, 3334.
- 12 S. Anderson, E. C. Constable, K. R. Seddon, J. E. Turp, J. E. Baggott and M. J. Pilling, *J. Chem. Soc., Dalton Trans.*, 1985, 2247.
- 13 R. J. Crutchley, N. Kress and A. B. P. Lever, *J. Am. Chem. Soc.*, 1983, **105**, 1170.
- 14 A. M. W. Cargill Thompson, J. C. Jeffery, D. J. Liard and M. D. Ward, *J. Chem. Soc., Dalton Trans.*, 1996, 879.
- 15 J. V. Caspar, B. P. Sullivan, E. M. Kober and T. J. Meyer, *Chem. Phys. Lett.*, 1982, **91**, 91.
- 16 S. R. L. Fernando and M. Y. Ogawa, *Chem. Commun.*, 1996, 637.
- 17 A. Juris, V. Balzani, F. Barigelletti, S. Campagna, P. Belser and A. Von Zelewsky, *Coord. Chem. Rev.*, 1988, **84**, 85.
- 18 G. F. Strouse, J. R. Schoonover, R. Duesing, S. Boyd, W. E. Jones and T. J. Meyer, *Inorg. Chem.*, 1995, **34**, 473.
- 19 J. G. Vos, *Polyhedron*, 1992, **11**, 2285.
- 20 A. Weller, *Prog. React. Kinet.*, 1961, **1**, 189.